

# Characteristics of Chatter Stability Lobe in 2-DOF Machining System

Hyuk Lee<sup>\*</sup>, Dohun Chin<sup>\*\*</sup>, Moonchul Yoon<sup>\*\*\*, #</sup>

<sup>\*</sup>Graduate school of Mechanical Design Engineering, PUKYONG NATIONAL UNIVERSITY

<sup>\*\*</sup>Department of Industrial Health, CATHORIC UNIVERSITY OF PUSAN

<sup>\*\*\*</sup>Department of Mechanical Design Engineering, PUKYONG NATIONAL UNIVERSITY

## 2-DOF 가공시스템의 채터로브 거동연구

이혁<sup>\*</sup>, 진도훈<sup>\*\*</sup>, 윤문철<sup>\*\*\*, #</sup>

<sup>\*</sup>부경대학교 대학원, <sup>\*\*</sup>부산가톨릭대학교 산업보건학과, <sup>\*\*\*</sup>부경대학교 기계설계공학과

(Received 5 May 2019; received in revised form 3 June 2019; accepted 7 June 2019)

### ABSTRACT

A chatter lobe analysis is frequently used to look at the chatter state [1-4]. Even if there is a lot of research on chatter, chatter lobe characteristics are not well defined. In this study, the chatter lobe behavior according to several variables of vibration mode is verified for further clarity. The dynamic variables of the chatter model are defined and their behaviors on chatter lobe boundary are analyzed in detail. In this sense, the chatter model with 2-DOF (2-DOF) was used to analyze chatter stability characteristics [4]. The discussed results are satisfying and these can be used for the prediction of chatter existence in machining processes of 2-DOF systems in several revolution range. These analyses indicate a better agreement for predicting an appropriate stability lobe over a wide detailed range of critical depths of cut in machining operation. The results allow an excellent prediction of chatter according to various static and dynamic variables in machining states. The behavior of chatter dynamic variables in machining were also discussed in detail. All these results can also be applied to other machining processes by establishing a chatter model in a 2-DOF system.

**Keywords** : Chatter Lobe(채터로브), Stability Region(안정영역), Transfer Function(전달함수)

## 1. Introduction

To better understand chatter behavior according to machining spindle speeds and depths of cut, the stability lobe using critical depth of cut, and spectrum analysis are frequently used in analysis of

the chatter model<sup>[1-10]</sup>. However, detailed chatter behavior according to the first and second vibration mode variables of 2-DOF (2-DOF) systems have not been verified clearly until now. To characterize the stability lobe of chatter, a dynamic variable such as natural frequency and the damping of chatter models must be verified, and its behavior was analyzed in this study. Therefore, the chatter model of 2-DOF systems was used to analyze chatter stability

# Corresponding Author : mcyoon@pknu.ac.kr

Tel: +82-51-629-6160, Fax: +82-51-629-6150

characteristics and to identify machining stability. The discussed results can be used for the prediction of chatter existence in a wide range of spindle speeds and depths of cut in the machining process. These results indicate a better agreement in obtaining appropriate stability boundary lobe behavior over a detailed range of spindle speeds and critical depths of cut. Finally, the results show an excellent prediction of chatter according to various static and dynamic variables in several chatter models. The behaviors of each dynamic variable of chatter in machining were also analyzed in detail. Each variable is supposed to influence the stability boundary and are proven to be realistic for changing the chatter stability boundary. With this study, chatter states are more easily discerned in cutting conditions by modeling in a 2-DOF system. Also, for easy prediction of boundary, the stability lobe boundary analysis program was developed by using a 2-DOF system; the results of each degree of model effect can be analyzed and be used later for easy prediction of stability lobe analysis. After all, their stability lobe boundaries can be displayed by using the developed program.

## 2. Chatter Analysis

### 2.1 Stability lobe of 2-DOF system

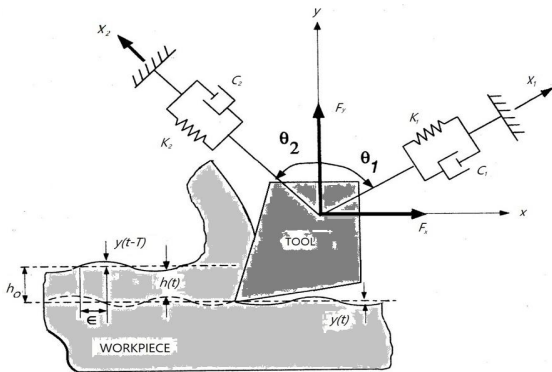


Fig. 1 Chatter model of a 2-DOF cutting system

The basic chatter model of a 2-DOF system is shown as in Fig. 1. It has stiffness and damping in each direction in the model. The transfer function,  $\Phi(j\omega)$ , of the chatter model may be summarized as follows<sup>[4]</sup>. In this case, an oriented structural transfer function of the model into the direction of chip thickness must be considered and the amplitude and phase of the vibration system are considered, respectively<sup>[4]</sup>.

$$\begin{aligned}
 |\Phi(j\omega)| &= \left| \frac{y(j\omega)}{F_y(j\omega)} \right| \\
 &= \cos^2\theta_1 \frac{1}{k_1} \left[ \frac{1-r_1^2}{\sqrt{(1-r_1^2)^2 + (2\zeta_1 r_1)^2}} \right] \\
 &\quad + \cos^2\theta_2 \frac{1}{k_2} \left[ \frac{1-r_2^2}{\sqrt{(1-r_2^2)^2 + (2\zeta_2 r_2)^2}} \right] \quad (1)
 \end{aligned}$$

$$\phi = \tan^{-1} \left( \frac{-2\zeta r}{1-r^2} \right) + \alpha \quad (2)$$

With the oriented transfer function, the negative real part of the complete transfer function around all dominant modes must be scanned using the same procedure as the cutting process. The machining process with a 2-DOF system is shown in Fig. 1, and the natural frequency and damping into the direction  $x_1$  and  $x_2$  may be given. The cutting force  $F_y = K_f a h(t)$  and the cutting constant  $K_f = 1.0 \times 10^6 \text{ N/m}^2$ , width of cut  $a$ , and depth of cut  $h(t)$  are given. The coordinate angle condition of  $\theta_1 = 30^\circ$  and  $\theta_2 = -45^\circ$  are each given respectively and these angles also move the boundary upward or downward. In this case, the real and imaginary FRF and stability lobe of the system can be plotted. The system flexibilities in directions  $x_1$  and  $x_2$ , may be obtained. Therefore, the real part of the oriented transfer function between the displacement in the  $y$ -direction and the cutting force  $F_y$  is obtained by Eq. (1), and the FRF of the real part, the imaginary part, and its power of oriented transfer function is given as Fig. 2.

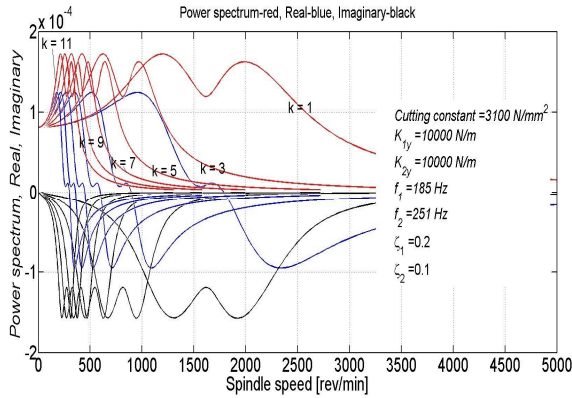


**Fig. 2 Predicted power, real, imaginary part of 2-DOF system**

Also, it shows the frequency response functions of real part  $G(w_c)$ , imaginary part  $H(w_c)$  and its power spectra in revolution range of machining according to integer  $k$  which is used in the solution of characteristic equation. From the characteristic equation, the following critical depth of cut may be summarized as Eq. 3<sup>[4]</sup>.

$$A_{lim} = \frac{-1}{2K_f G(w_c)} \quad (3)$$

By substituting the real part,  $G(w_c)$ , the boundary of stability lobe can be obtained according to several variables such as cutting constant, stiffness, and damping into  $x$  and  $y$  direction. The stability lobe is configured as Fig. 3; it may be obtained by superposing all the boundaries-the lowest corresponding stability boundary can be configured. And the stability lobes are obtained with blue line boundary as in Fig. 3. The effect of  $K_c$ , which is correlated with a workpiece material, must be investigated in the lobe boundary with different cutting constant as in Fig. 4.

Fig. 4 shows a stability lobe boundary according to cutting constant of a machining system with some

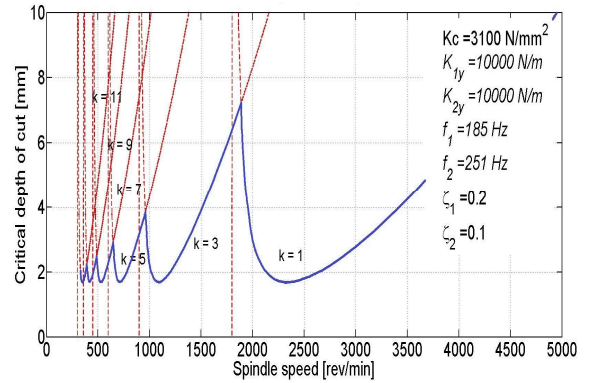


**Fig. 3 Predicted stable boundary curve of a 2-DOF system**

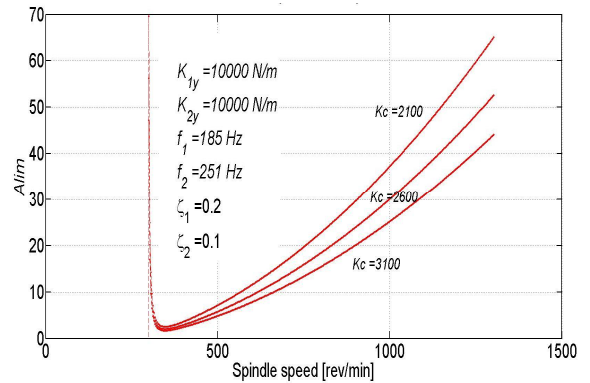
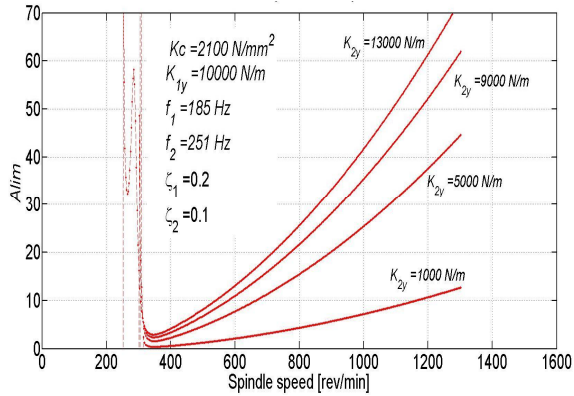


**Fig. 4 Stability boundary curve according to cutting constant  $K_c$**

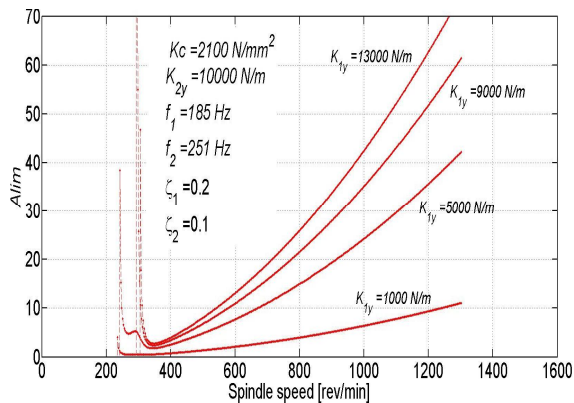
material. As cutting constant( $K_c$ ) increases, the stable region decreases because of the strong force in the same stiffness machining condition. Fig. 4 shows a stability lobe boundary according to different cutting constants. As a cutting constant  $K_c$  increases in general, the stable region becomes wider and lower as in Fig. 4. The different detailed behaviors of boundary shape were obtained by solving the characteristic equation and it may be discussed in the figures. The machining system has stiffness in each direction for a 2-DOF system. Therefore, each of its effects on stability boundary may change and it must be investigated in detail. Fig. 5(a) and Fig. 5(b) show

stability lobe boundaries according to the 1<sup>st</sup> and 2<sup>nd</sup> modes of stiffness. As the stiffness of each of the first and second modes increase, the boundary moves upward, and the unstable region increases and becomes wider in the right side. In Fig. 5(a) and Fig. 5(b), the stability lobe boundaries according to stiffness of the 1<sup>st</sup> and 2<sup>nd</sup> modes are shown in detail in their respective figures.

As stiffness of each mode increases, both stable regions increase too. Furthermore, the different shapes of double convex behavior downward appear for lower stiffness in the given spindle revolution range.



(a) Stability boundary according to stiffness  $K_{y_1}$



(b) Stability boundary according to stiffness  $K_{z_1}$

**Fig. 5 Stability region according to variables of chatter condition**

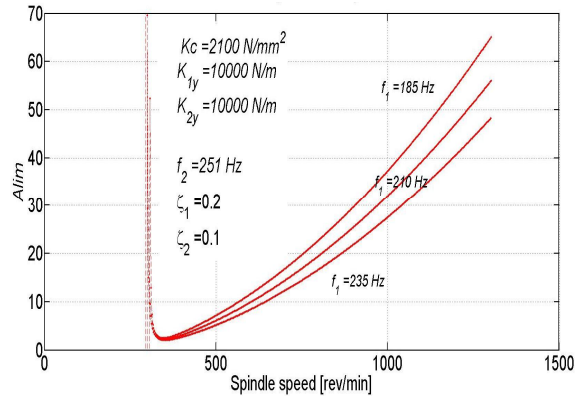


**Fig. 6 Stability boundary according to 1<sup>st</sup> mode frequency,  $f_1$ .**

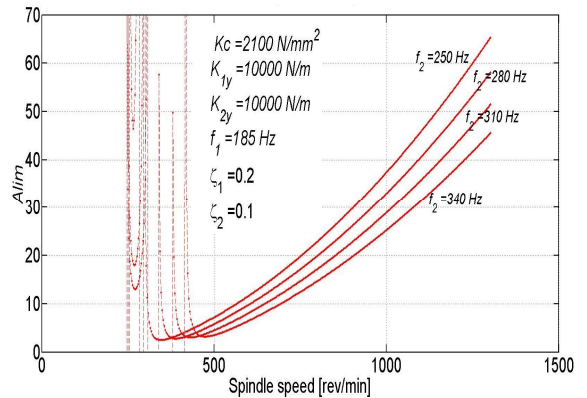


**Fig. 7 Stability boundary according to 2<sup>nd</sup> mode frequency,  $f_2$ .**

The effect of mode frequency was also investigated in this study and their behaviors also appear in the case of lower damping ratios for the 1<sup>st</sup> and 2<sup>nd</sup> modes in Fig. 8 and Fig. 9, respectively. The given machining system has natural frequency and damping in each direction. The mode frequency and damping in each mode also have some effect on the stability boundary and it must also be investigated. Therefore, their effects on the stability lobe boundary was investigated in detail. Fig. 6 shows the stability lobe boundary of the 1<sup>st</sup> mode of natural frequency. As the natural frequency of

the 1<sup>st</sup> mode increases, the unstable region decreases into the downward right region too. It means that a higher natural frequency of the 1<sup>st</sup> mode causes a wider unstable region in the lobe boundary; therefore, it is necessary to have a lower natural frequency in the system to get a wider stable region same as the other given conditions.

Fig. 7 also shows stability lobe boundary according to the 2<sup>nd</sup> mode frequency. As the 2<sup>nd</sup> mode frequency increases, the stable region decreases downward. Therefore a higher natural frequency in the 2<sup>nd</sup> mode may also cause a smaller unstable region in the lobe. It also moves the boundary curve downward and incurs a wider stable region. And it is necessary to have higher natural frequency to get a wider stable region in the same condition. Fig. 6 and Fig. 7 show the stability lobe boundary according to 1<sup>st</sup> and 2<sup>nd</sup> mode respectively. As the natural frequency of each mode increases, the stable region, in both cases, increases into a downward convex shape.

The damping effect on stability boundaries was investigated in Fig. 8 and in Fig. 9. Fig. 8 shows a stability lobe boundary according to damping of the 1<sup>st</sup> mode. The damping of 1<sup>st</sup> mode also influences stability boundary. As the damping of 1<sup>st</sup> mode increases, the boundary moves upwards, and the stable region increases too. However, different behavior of the right-side lobe shape appears for the first damping,  $\zeta_1$ , in the solution of the characteristic equation for the low integer  $k = 3$ . A further boundary of higher  $k$  can be generated in the left side successively, and each boundary can be generated as shown by superposing as in Fig. 8. It also shows a stability lobe boundary of a 2-DOF chatter system. The lobe for  $k = 1$  appears in right-side at a higher revolution, ranging up above 1450 rpm, in figure according to 1<sup>st</sup> damping  $\zeta_1$ . The lower damping decreases the stable region and it moves the lobe boundary downwards in each revolution range. Also, by considering all the

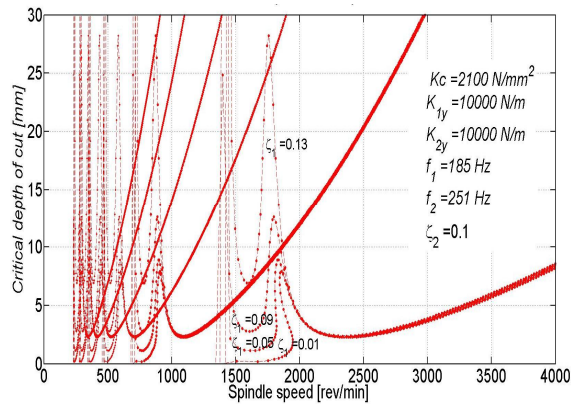


Fig. 8 Approximate stability lobe behavior according to damping

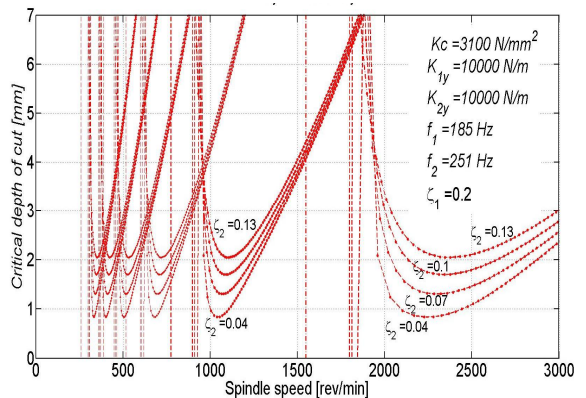


Fig. 9 Approximate stability lobe behavior according to damping.

solutions of the characteristic equation, at an integer for  $k = 1$  to  $k = 7 \dots$ , it can discriminate between the stable region and unstable one. The stability lobe boundary may be configured by supposing the boundaries by selecting the lowest boundary line. The effect of the 2<sup>nd</sup> mode of damping on stability boundaries has also been investigated in detail. Fig. 9 shows a stability lobe boundary of a chatter model of a 2-DOF system according to the 2<sup>nd</sup> mode damping  $\zeta_2$ . The higher second damping also increases the stability region in the revolution range as in Fig. 9, but the shape of Fig. 9 is a little bit

different compared to Fig. 8 which shows the 1st mode boundary.

Comparing to the 1<sup>st</sup> mode damping, the stable boundaries of the 2<sup>nd</sup> mode of damping decreases the stable region of a boundary in a simpler shape. A lower 2<sup>nd</sup> mode of damping also moves boundary downwards in the revolution range and this can be seen clearly in Fig. 9. Considering all cases of integer  $k = 1$  to  $k = 7 \dots$ , the lobe boundary may be configured in the lowest trajectory by superposing each curve. By superposing each curve, the total stable region boundary can be configured completely. The completed stable region is seen in Fig. 9.

Fig. 10(a) shows a final stability lobe boundary of a chatter model of a 2-DOF system. The lobe of integer  $k = 1$  appears in a higher revolution, ranging up above 1800 rpm in Fig. 10(a). The lobe of integer  $k = 2$  appears in the revolution ranging above 1200 rpm to 3000 rpm in Fig. 10(a). For the integer  $k = 3$ , the lobe boundary only appears above 900 rpm. Considering all integers  $k = 1$  to  $k = 7 \dots$ , the lobe boundary may be configured in a blue line as in Fig. 10(a). However, Fig. 10(b) shows the final stability lobe boundary of a chatter model in different conditions of smaller first damping (for  $\zeta_1=0.05$ ) than that(for  $\zeta_1=0.2$ ) of Fig.10(a). The lobe of integer  $k = 1$  appears in higher revolutions ranging up above 1350 rpm in Fig. 10(b). The lobe of integer  $k = 2$  appears in the revolution ranging above 900 rpm to 3000 rpm in Fig. 10(b). Also, for the integer of  $k = 3$ , the lobe boundary only appears above 700 rpm. Considering all integers for  $k = 1$  to  $k = 7 \dots$ , the lobe boundary may be configured in a blue downward line as Fig. 10(b). In these figures, it is shown that the stability region of Fig. 10(a) for  $\zeta_1=0.2$ , is wider than Fig. 10(b) for  $\zeta_1=0.05$ . Therefore, the increased critical depth of cut in a stable state can be accomplished by increasing 1st damping appropriately. By decreasing the damping ratio,  $\zeta_1$ , of the 1st mode, the lobe of the stable region may

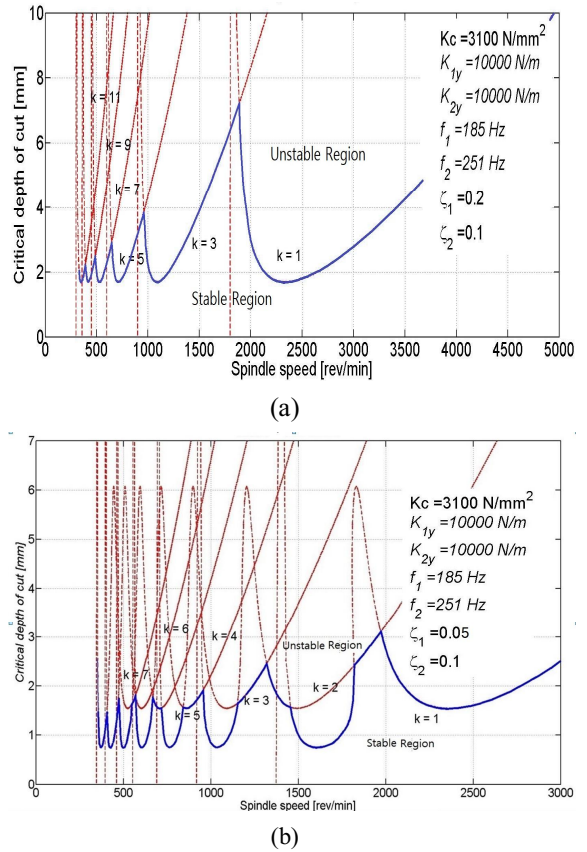


Fig. 10 Approximate stability lobe behavior

change from Fig. 10(a) to Fig. 10(b) as shown. It shows that a stable region of a larger depth can exist in small damping. If the appropriate revolution is selected in machining considering these phenomena, and for  $k = 1$ , a double convex lobe boundary downward may appear as Fig. 10(b). Therefore, all phenomena may be superimposed, and the final boundary may be generated in every range of revolution.

### 3. Conclusion

In this study, the chatter characteristics of 2-DOF machining systems were evaluated by investigating the stable boundary curve and the following

conclusions were drawn:

1. According to various dynamic chatter variables, the stability behavior was investigated in detail. The lobe boundary and stability regions can be characterized clearly according to stiffness, 1st and 2nd modes damping, and the natural frequencies of 2-DOF chatter models in this study.
2. Small damping of 1st mode causes an irregular stability boundary in lobes because it supposes twin lobe boundaries at each integer  $k$  of the characteristic equation.
3. These results can be extended to characterize a detailed stable boundary region in machining operation in a wide range of cutting conditions considering both static and dynamics variables.

## References

1. Tobias, S. A. and Fishwick, W., "The Chatter of Lathe Tools under Orthogonal Cutting Conditions", Transactions of ASME, Vol. 80, pp. 1079-1088, 1958.
2. Tlustý, J. and Poláček, M., "The stability of machine tools against self-excited vibrations in machining", Proceedings of the International Research in Production Engineering Conference, Pittsburgh, PA, New York, pp. 465-474, 1963.
3. Meritt, H. E., "Theory of self-excited machine tool chatter", Transactions of the ASME, Journal of Engineering for Industry 87, pp. 447-454, 1965.
4. Altintas, Y., Manufacturing Automation, Cambridge Univ. Press, 2000.
5. Oh, S. L., Chin, D. H., Yoon, M. C., Ryoo, I. I. and Ha, M. K., "Chatter Mode and Stability Boundary Analysis in Turning", Journal of the Korean Society of Manufacturing Technology Engineers, Vol. 14, No.5, 2005.
6. Yoon, M. C., Cho, H. D. and Kim, S. K., "A Study on Diagnostics of Machining System with ARMA Modeling and Spectrum Analysis", Journal of the Korean Society of Manufacturing Technology Engineers, Vol. 8, No. 3, pp. 42-51, 1999.
7. Chin, D. H., Yoon, M. C., Yoon, S. K., and Cho, H. D., "Spectral analysis of malfunction mode in end-milling", J. of Mechanical Science and Technology, Vol. 21, pp. 1637-1643, 2007.
8. Kim, J. D. and Yoon, M. C. "Parametric modelling of uncoupled system", Journal of the Korean Society of Manufacturing Process Engineers, Vol. 5, No. 3, pp. 36-42, 2006.
9. Kim, J. D. and Yoon, M. C., "Mode analysis of end-milling process by REIVM", KSMTE Autumn Conference, pp. 414-419, 2010.
10. Oh, S. L., Chin, D. H. and Yoon, M. C. "Detection and Analysis of Chatter in End-milling Operation", Journal of the Korean Society of Manufacturing Technology Engineers, Vol. 13, No. 6, pp. 10-16, 2004.